# Noninvasive Assessment of the Right Ventricular Filling Pressure Gradient

Cristina Cortina, MD; Javier Bermejo, MD, PhD; Raquel Yotti, MD, PhD; M. Mar Desco, MD, PhD; Daniel Rodríguez-Pérez, PhD; J. Carlos Antoranz, PhD; José Luis Rojo-Álvarez, MEng, PhD; Damien Garcia, Eng, PhD; Miguel A. García-Fernández, MD, PhD; Francisco Fernández-Avilés, MD, PhD

***Background***—The physiological basis of right ventricular (RV) diastolic function remains incompletely studied in humans. The driving force responsible for RV filling, the pressure gradient along the RV inlet from the right atrium to the RV apex, has never been measured in the clinical setting.

***Methods and Results***—We validated a method for measuring the RV filling pressure difference (RVFPD) from color Doppler M-mode recordings in 12 pigs undergoing interventions on RV preload, afterload, and lusitropic states (error, $-0.1 \pm 0.4$ mm Hg compared with micromanometers; intraclass correlation coefficient, 0.88). Peak early RVFPD correlated directly with mean right atrial pressure and inversely with the time constant of RV relaxation. In 21 patients with dilated cardiomyopathy, the peak RVFPD was 1.0 mm Hg (95% CI, 0.8 to 1.2), significantly lower than in age-matched control subjects (1.4 mm Hg; 95% CI, 1.2 to 1.6). In another population of 19 young healthy volunteers, the peak RVFPD was 2.3 mm Hg (95% CI, 2.0 to 2.6), which was reduced by nitroglycerine and esmolol and was augmented by volume overload and atropine infusions. RVFPD was generated almost exclusively by inertial forces.

***Conclusions***—For the first time, the RV driving filling force can be accurately measured noninvasively in the clinical setting, and the method is sensitive to detect the effects of preload, chronotropic, and lusitropic states. In patients with dilated cardiomyopathy, the RV filling force is markedly reduced, indicating severely impaired RV relaxation. These findings suggest that this is a useful tool for improving the clinical assessment of RV diastolic function. **(*Circulation*. 2007;116:1015-1023.)**

**Key Words:** diastole ■ echocardiography ■ hemodynamics ■ ventricles ■ imaging ■ pressure

Right ventricular (RV) dysfunction is known to adversely affect prognosis in patients with a number of cardiovascular disease states.[1] Additionally, RV function plays a major role in normal and abnormal cardiopulmonary interactions.[2,3] However, most research has focused on RV systolic function; the diastolic properties of the RV remain scarcely studied in patients. Well-characterized diastolic properties of the left ventricle (LV) such as relaxation have only been incompletely studied in the right heart, almost never in the clinical setting.[4–7]

## Clinical Perspective p 1023

The driving force for RV filling is the diastolic pressure gradient along the RV inlet, from the right atrium (RA) to the RV apex. To date, the RV filling pressure difference (RVFPD) between these 2 locations can be measured only by sophisticated high-fidelity catheterization procedures or complex functional 3-dimensional imaging methods, which are clinically unavailable.[5–7] To the best of our knowledge, not even the magnitude of the physiological RVFPD has ever been reported for the human heart.

The analysis of the pressure difference along the LV inflow tract has provided crucial insight into LV filling. Briefly, in the presence of a normal valve, the LV filling pressure difference is determined principally by left atrial pressure and the rate of LV relaxation.[8,9] Although it has been hypothesized that similar factors determine the RVFPD,[10] this issue has never been specifically addressed. If left-side equivalents hold for the right side of the heart, measuring the RVFPD could be a clinically useful tool to assess RV diastolic function because RA pressure can be accurately estimated noninvasively.

Recently, the possibility of measuring intracardiac pressure gradients by digital processing of color Doppler M-mode

Received January 18, 2007; accepted June 26, 2007.

From the Department of Cardiology (C.C., J.B., D.G., M.A.G.-F., F.F.-A.) and the Unit of Experimental Medicine and Surgery (M.M.D.), Hospital General Universitario Gregorio Marañón, Madrid, Spain; Department of Mathematical Physics and Fluids (D.R.-P., J.C.A.), Facultad de Ciencias, Universidad Nacional de Educación a Distancia, Madrid, Spain; and the Department of Signal Theory and Communications (J.L.R.-A.), Universidad Rey Juan Carlos, Madrid, Spain.

Presented in part at the 2006 American Heart Association Scientific Sessions, Chicago Ill, November 4–7, and published in abstract form (*Circulation*. 2006;114[suppl II]:II-363).

Correspondence to Javier Bermejo, MD, PhD, Department of Cardiology, Hospital General Universitario Gregorio Marañón, Dr Esquerdo 46, 28007 Madrid, Spain. E-mail javbermejo@jet.es

© 2007 American Heart Association, Inc.

*Circulation* **is available at http://circ.ahajournals.org** **DOI: 10.1161/CIRCULATIONAHA.107.691154**

images has been developed by our[11–14] and other groups.[15,16] We hypothesized that this method also could be suitable for measuring the RVFPD in clinical practice.

The present study was designed to test the reliability and clinical applicability of measuring the RVFPD by digital processing of color Doppler M-mode recordings. First, the method was validated using high-fidelity micromanometers in an animal experimental model, which also was used to assess the hemodynamic factors that determine the magnitude of the RVFPD. The noninvasive method was then used to compare the RVFPD of patients with dilated cardiomyopathy (DCM) with age-matched control subjects. Finally, the sensitivity of the method to assess the effects of interventions on preload, lusitropy, and filling time on the RVFPD was studied in a population of young healthy volunteers.

## Methods

### Animal Experimental Protocol and Data Analysis

The study protocol was approved by the local Institute Care Committee. Twelve minipigs (weight, 57±7 kg; Instituto Madrileño de Investigación y Desarrollo Rural, Agrario y Alimentario, Madrid, Spain) were studied in a closed-chest instrumentation setup. Animals were preanesthetized with ketamine and xylazine and mechanically ventilated. Complete anesthesia and relaxation were obtained by repetitive boluses of pentobarbital (15 mg/kg IV plus 5 mg · kg$^{-1}$ · 15 min$^{-1}$) and pancuronium (0.2 mg/kg). Blood gases were measured at 15- to 30-minute intervals, and the ventilator was adjusted accordingly. Animals were euthanized at the end of the experiments.

Micromanometer catheters (Millar Instruments Inc, Houston, Tex) were placed in the RA and RV through the right jugular and right femoral veins, respectively. To avoid drift and to eliminate hydrostatic pressure differences, micromanometers were balanced in vivo for equal pressure during a long diastasis after a premature beat.[17] To ensure temporal matching of Doppler echocardiography and invasive data, a synchronization signal was simultaneously fed into the ultrasound scanner and the data acquisition system and then retrospectively matched by cross-correlation. Pressure, synchronicity, and ECG signals were digitized at 500 Hz on a Pentium III computer with custom-built amplifiers, a 16-channel analog-to-digital converter board, and virtual instrumentation software.

Combined interventions on RV preload, afterload, and relaxation were performed to obtain a wide range of RVFPD values. Preload was acutely modified by intravenous infusion of nitroglycerine (160 to 600 μg/min; n=5) and saline (n=4). Additionally, a high-output left-to-right peripheral shunt connecting a 22F cannula between left main femoral artery and vein was created in 3 pigs. Flow across the fistula was monitored by a transit-time Doppler system (Transonics, Ithaca, NY) and adjusted manually from 300 to 1200 mL/min; volume expansion was used to increase preload further in these animals. In 3 pigs, controlled acute pulmonary hypertension was induced by repeated intravenous boluses (0.5 mg) of *Escherichia coli* endotoxin (LPS 0127:B8, Sigma Chemical, St Louis, Mo) titrated according to RV pressure and hemodynamic stability. Relaxation rate was modified by esmolol (500 μg/kg bolus, followed by 50- to 200-μg · kg$^{-1}$ · min$^{-1}$ infusion; n=9).

The RVFPD curve was obtained as the instantaneous difference of absolute RV-RA pressures. Additionally, values of mean RA pressure, peak systolic RV pressure, peak RV $dP/dt_{max}$, and $-$RV $dP/dt_{min}$ were obtained from the micromanometric data. The time constant of relaxation ($\tau$) was obtained with a monoexponential RV model by nonlinear regression fitting the RV pressure decay data from the time of $-dP/dt_{min}$ to 3 mm Hg above the subsequent end-diastolic pressure.[18]

### Human Population and Clinical Protocol

Twenty-three patients with DCM, 23 age-matched control subjects, and 20 young healthy volunteers were included. Images from 2 patients, 2 control subjects, and 1 young volunteer were unsuitable for analysis. Therefore, 21 patients, their 21 control subjects (healthy subjects matched by sex and age), and 19 young volunteers constitute the basis of this report. The last 2 populations were not on any medication, and cardiovascular disease was ruled out by history, clinical examination, ECG, and Doppler echocardiography. In young healthy volunteers, images were taken at baseline and during infusion of esmolol (500 μg/kg bolus, followed by increasing infusion from 50 to 200 μg · kg$^{-1}$ · min$^{-1}$ in steps of 50 μg · kg$^{-1}$ · min$^{-1}$ every 5 minutes), saline (1000 mL in 15 to 30 minutes), nitroglycerine (5 to 200 μg/min in steps of 10 μg/min titrated on the basis of blood pressure), and atropine (1 mg). Recordings were obtained during steady hemodynamic state, and each drug was followed by a 15-minute washout period.

Stable DCM patients were referred from the heart failure outpatient clinic. In this group, LV end-diastolic volume was 148±48 mL (biplane Simpson's method), LV ejection fraction was 0.35±0.10, systolic pulmonary arterial pressure was 38±21 mm Hg, and origin was proven ischemic heart disease in 16 (71%) and idiopathic in 5 (29%). Tricuspid annular plane systolic excursion was 16±5 mm in patients, lower than in control subjects (23±3 mm; $P<0.001$).[19] In DCM patients, tricuspid regurgitation was absent in 7 patients, mild in 13, and moderate in 1; estimated RA pressure was 5 to 10 mm Hg in all patients except 1.[20] The study protocol was approved by the institutional ethics committee, and written informed consent was obtained from all subjects.

### Echocardiographic Image Acquisition and Analysis

Broadband transducers (2.0 to 4.0 MHz) were used on a Vivid 7 (GE Ultrasound, Horten, Norway) and a Sequoia C-256 ultrasound system (Siemens AG, Munich, Germany). Images were obtained from an anteriorly modified 4-chamber apical view through either a subxifoid abdominal incision (animals) or a transthoracic approach (humans). Care was taken to align the M-mode cursor with the RV filling flow as visualized by 2-dimensional color Doppler. Pulse repetition frequency was adjusted to visualize the low-velocity flow of RV filling with maximum sensitivity. Animal images were taken during transient disconnection to the ventilator; clinical images were taken during end-expiration apnea.

The method used for digital image processing of color M-mode Doppler echocardiograms has been described.[11–13] Briefly, if the M-mode cursor closely approximates a flow streamline, the spatiotemporal velocity distribution of a discrete blood sample is provided by the value of its corresponding pixel color: $v(s,t)$, where v represents velocity, s represents the linear dimension of the streamline, and t is time. Thus, the color M-mode Doppler recording provides the data necessary to solve Euler's momentum equation:

$$\frac{\partial p}{\partial s} = -\rho \cdot \left( \underbrace{\frac{\partial v}{\partial t}}_{\text{Inertial}} + \underbrace{v \cdot \frac{\partial v}{\partial s}}_{\text{Convective}} \right), \quad (1)$$

where p is pressure and $\rho$ is blood density. The first term on the right side of the equation designates inertial (local) acceleration; the second term accounts for convective (spatial) acceleration.[13] Gradients are displayed as color overlays representing the pressure difference between 1 pixel and another pixel located 1 cm closer to the transducer (in mm Hg/cm; Figure 1).

Instead of using fixed distances between stations, we placed the positions of the RA and the RV apex on the basis of the images, attempting to match catheter positions in the animal validation study.[11,13] RVFPD curves were calculated by spatial integration of gradient maps between these 2 stations. Onset and end of the filling flow were determined visually from the raw color Doppler M-mode image. In figures and tables, the temporal reference was established at QRS onset. Temporal measurements are normalized to filling time. Four to 9 consecutive beats were measured in the clinical study for each hemodynamic stage.

The following parameters were measured from the RVFPD curves: peak early, peak late, time to peak early, time to peak late, and mean (time-averaged) RVFPD. Intraobserver, interobserver, and beat-to-beat reproducibilities (30 beats from the clinical data set blindly measured

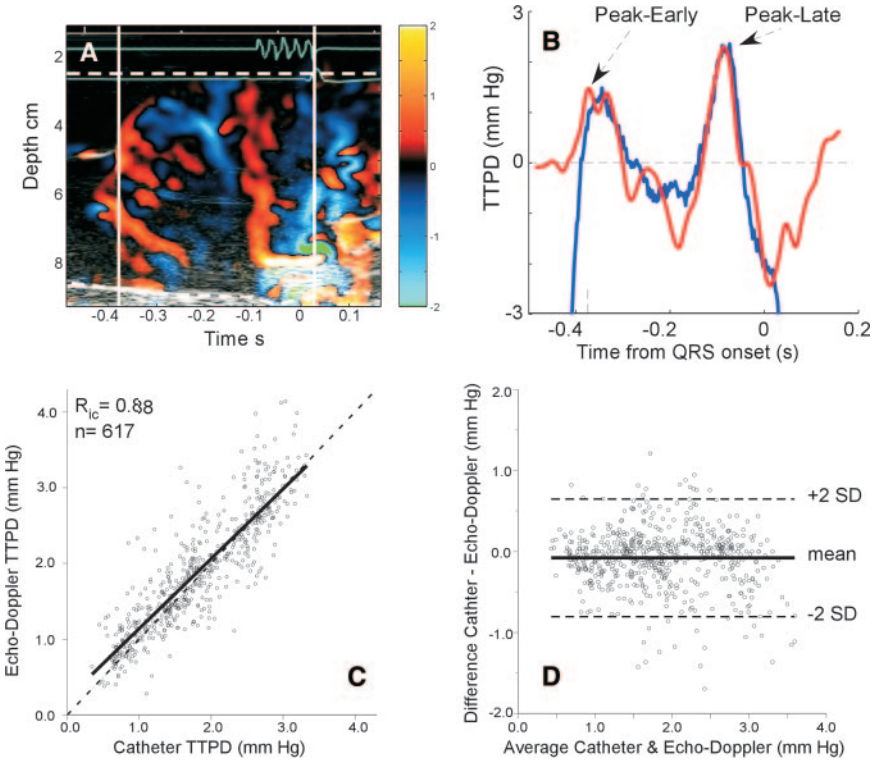


**Figure 1.** Experimental validation analysis. A, RV filling pressure gradient image from a representative example. Colors represent the pressure difference between each pixel and another located 1 cm closer to the transducer (mm Hg/cm). Micromanometer positions at the RV apex and high RA are overlaid as white dotted lines. B, Curves obtained by echo-Doppler (red) and micromanometers (blue). C and D, Correlation and Bland-Altman analyses.

>3 months apart) of the noninvasive peak early RVFPD were 0.0±0.1 (−1±6%), 0.0±0.2 (1±5%), and 0.1±0.3 mm Hg (4±14%), respectively. Beat-to-beat variability of the invasive peak early RVFPD measurement was 0.0±0.2 mm Hg (0±12%).

## Statistical Analysis

Quantitative variables are expressed as mean±SD. Validation and method variabilities were analyzed with the intraclass correlation coefficient and Bland-Altman analyses. Comparisons between subject groups (paired and unpaired designs as appropriate) and the effects of hemodynamic interventions and determinants of RVFPDs (repeated-measures designs) were analyzed by linear and nonlinear mixed-effects models, respectively (S-Plus version 6.1, Insightful Corp, Seattle, Wash). Fixed-effect coefficients and their 95% CIs are reported for these models. Fixed-effect coefficients account for the mean expected values of variables once the source of variation resulting from the animal/subject sampling random effect is omitted. Significant linear mixed-effects models were followed by simulation contrasts.[21] Values of $P<0.05$ were considered significant.

The authors had full access to and take full responsibility for the integrity of the data. All authors have read and agree to the manuscript as written.

# Results

## Animal Studies

Hemodynamic interventions induced a wide range of variations of RV preload, afterload, and $\tau$ (Table 1). Despite these

**TABLE 1. Effects of Hemodynamic Interventions in the Animal Study**

| | | Preload | | Afterload | Relaxation |
|---|---|---|---|---|---|
| | Baseline | Nitroglycerine | Volume Overload | Endotoxin | Esmolol |
| Beats, n | 129 | 29 | 159 | 179 | 121 |
| Animals, n | 12 | 5 | 7 | 3 | 9 |
| Heart rate, bpm | 90 (84 to 96) | 77 (71 to 83)* | 70 (65 to 76)* | 77 (71 to 83)* | 74 (69 to 80)* |
| Filling time, ms | 249 (213 to 285) | 319 (278 to 359)* | 364 (327 to 401)* | 264 (225 to 303) | 368 (331 to 404)* |
| Mean RA pressure, mm Hg | 6.1 (4.9 to 7.3) | 5.1 (3.7 to 6.5) | 12.1 (10.9 to 13.3)* | 4.3 (2.9 to 5.6)* | 8.3 (7.1 to 9.5)* |
| Minimum RV diastolic pressure, mm Hg | 3.8 (2.5 to 5) | 2.3 (0.9 to 3.7)* | 8.9 (7.6 to 10.1)* | 4.8 (3.4 to 6.2)* | 5.8 (4.5 to 7)* |
| End-diastolic RV pressure, mm Hg | 8.8 (7.5 to 10.1) | 8.4 (6.9 to 9.9) | 15.6 (14.3 to 16.9)* | 8.0 (6.6 to 9.4) | 11.1 (9.8 to 12.4)* |
| Peak-systolic RV pressure, mm Hg | 33.8 (31.4 to 36.3) | 31.4 (27.7 to 35.1) | 38.1 (35.5 to 40.7)* | 43.9 (40.8 to 46.9)* | 32.3 (29.7 to 34.8) |
| RV $dP/dt_{max}$, mm Hg/s | 682 (584 to 779) | 510 (388 to 632)* | 522 (420 to 623)* | 644 (533 to 755) | 496 (396 to 596)* |
| RV $\tau$, ms | 58 (47 to 69) | 56 (43 to 68) | 84 (73 to 95)* | 59 (47 to 71) | 65 (54 to 76)* |
| RV $-dP/dt_{min}$, $-1 \cdot$ mm Hg/s | 425 (362 to 489) | 428 (357 to 499) | 365 (300 to 430)* | 598 (530 to 665)* | 376 (312 to 441)* |
| Peak early RVFPD, mm Hg | 2.1 (1.8 to 2.4) | 2.2 (1.9 to 2.6) | 1.8 (1.5 to 2.2)* | 1.8 (1.5 to 2.2)* | 1.7 (1.4 to 2.1)* |

Values show the estimated fixed effects (95% CI) from mixed models controlling for repeated measures within animal.
*$P<0.05$ vs baseline.

**TABLE 2. Validation of the Noninvasive RVFPD Measurements**

| | Absolute Error | Relative Error | $R_{ic}$ | SEE |
|---|---|---|---|---|
| Peak early RVFPD, mm Hg | −0.1±0.4 | 5±22 | 0.88 | 0.34 |
| Peak late RVFPD, mm Hg | 0.1±0.4 | −3±23 | 0.78 | 0.41 |
| Time to peak early, ms | 0±19 | 0±8 | 0.97 | 18 |
| Time to peak late, ms | 2±11 | -3±22 | 0.83 | 11 |

$R_{ic}$ indicates intraclass correlation coefficient; SEE, standard error of the estimate.

hemodynamic changes, RVFPD remained relatively stable in the 1.5- to 2.5-mm Hg range. Close agreement was observed between the noninvasive method and micromanometers to estimate the peak early and late RVFPD (Table 2 and Figure 1). By multivariate analysis, both mean RA pressure and $\tau$ correlated with peak RVFPD (Table 3 and Figure 2). However, the relationship between mean RA pressure and RVFPD was highly nonlinear, fitting a quadratic regression model. Baseline mean diastolic values of RVFPD obtained by invasive and noninvasive methods were 0.0 mm Hg (95% CI, −0.4 to 0.5) and −0.1 mm Hg (95% CI, −0.3 to 0.0), respectively, and these values were not significantly different from 0 at baseline ($P=0.9$ and $P=0.1$, respectively, for each method) or during any hemodynamic intervention ($P>0.09$ for all).

## Assessment of the RVFPD in Humans: Effects of Hemodynamic Interventions

The peak early RVFPD was significantly lower in DCM patients than in age-matched control subjects. In turn, it was lower in age-matched control subjects than in young healthy volunteers (Table 4 and Figure 3). These differences were due to differences in the inertial component. Significant hemodynamic changes were induced by the pharmacological interventions in volunteers. Peak early RVFPD decreased significantly during the infusion of nitroglycerine and esmolol, whereas it increased during volume overload and atropine (Figure 4); additional changes in other RVFPD curve parameters were observed (Table 4). The peak early RVFPD was almost completely determined by its inertial component. There was no contribution of convective forces resulting from the opposite effects of flow acceleration toward the tricuspid inlet and deceleration once inside the ventricle (Figure 5). Changes in E-wave flow velocity followed changes in the early RVFPD, although the slope of this relationship was highly variable among subjects (Figure 6). In DCM patients and their control subjects, correlation between peak early RVFPD and tricuspid annular plane systolic excursion was $R=0.3$ ($P=$NS); there was a negative significant correlation

**TABLE 3. Hemodynamic Determinants of the RVFPD**

| Variable | Fixed Effect (95% CI) | P |
|---|---|---|
| Mean RA pressure | −0.08 (−0.17 to 0.01) | 0.07 |
| Squared mean RA pressure | 0.004 (0.001 to 0.008) | 0.01 |
| RV $\tau$ | −0.009 (−0.016 to −0.004) | 0.002 |
| Intercept | 2.8 (2.1 to 3.5) | <0.0001 |

Data are from animals undergoing interventions on preload and relaxation. Overall within-animal regression coefficient=0.80.

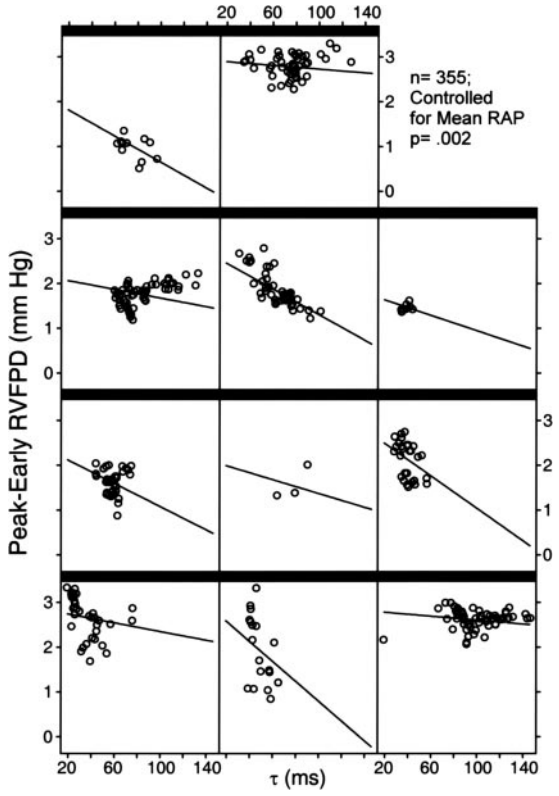


**Figure 2.** Time constant of RV relaxation ($\tau$) as a determinant of the RVFPD in the animal experiments. Data from each animal are plotted individually for baseline, preload, and relaxation interventions. RAP indicates RA pressure.

of the peak early RVFPD with age ($R=-0.48$; pooled normal control populations, $P<0.05$).

## Discussion

To the best of our knowledge, our study provides, for the first time in humans, values of the diastolic RVFPD. Furthermore, our study demonstrates the feasibility and accuracy of a method for obtaining these measurements noninvasively, allowing investigators to characterize the driving pressure responsible of RV filling in the clinical setting. The fact that RV early diastolic pressure was negative and lower than RA pressure was first described by Sabbah et al[22] and Sabbah and Stein[23] using micromanometers in pigs and humans. Measurements of the RVFPD have been reported in dogs by Courtois et al.[24] In their study, the early RVFPD was 1.6±0.5 mm Hg, a value very close to our results, although their measurement of the early RVFPD was computed as a nonsimultaneous difference between the RA and RV pressure curves instead of the peak instantaneous value we used in our study.

Classical studies using fluid-filled catheters have identified a mean pressure difference >1.9 mm Hg at rest or 2.0 mm Hg during exercise as highly diagnostic of tricuspid stenosis in patients with rheumatic heart disease.[25] This observation is accordant with our results showing that, in the presence of a completely normal tricuspid valve, the mean RVFPD must be very close to 0 mm Hg when measured between the high RA and the RV apex.

**TABLE 4. Clinical Study**

| | DCM, Baseline | Age-Matched Control Subjects, Baseline | Young Healthy Volunteers | | | | |
|---|---|---|---|---|---|---|---|
| | | | Baseline | Nitroglycerine | Volume | Esmolol | Atropine |
| Age, y | 66±12 | 66±10¶ | | | 28±5 | | |
| Gender, M/F | 15/6 | 15/6 | | | 8/11 | | |
| Weight, kg | 70±11 | 72±10 | | | 66±11 | | |
| Heart rate, bpm | 64 (59 to 70) | 67 (61 to 73) | 68 (63 to 72) | 68 (64 to 73) | 69 (65 to 73) | 61 (57 to 65)# | 89 (85 to 93)# |
| Systolic blood pressure, mm Hg | 125 (115 to 135) | 132 (122 to 142)¶ | 115 (110 to 119) | 99 (95 to 103)# | 110 (106 to 115)# | 99 (95 to 103)# | 112 (108 to 117) |
| Diastolic blood pressure, mm Hg | 77 (71 to 84)§ | 80 (73 to 86)¶ | 64 (60 to 67) | 46 (43 to 50)# | 56 (53 to 60)# | 52 (48 to 55)# | 59 (56 to 62)# |
| Filling time, ms, | 548 (368 to 729) | 557 (478 to 637) | 620 (553 to 687) | 548 (480 to 617) | 512 (444 to 580)# | 614 (546 to 682) | 362 (293 to 432)# |
| Relative filling time, % | 55 (35 to 75) | 54 (42 to 67) | 68 (61 to 75) | 61 (54 to 68) | 58 (51 to 65) | 62 (55 to 69) | 50 (43 to 58)# |
| RV filling peak E-wave velocity, cm/s | 28 (25 to 32)§ | 31 (27 to 34)¶ | 56 (52 to 60) | 53 (49 to 57) | 66 (61 to 70)# | 53 (49 to 57) | 62 (57 to 66)# |
| RVFPD data | | | | | | | |
| Peak early RVFPD, mm Hg | 1.0 (0.8 to 1.2)†§ | 1.4 (1.2 to 1.6)¶ | 2.3 (2.0 to 2.6) | 1.8 (1.6 to 2.1)# | 2.6 (2.3 to 2.9)# | 2.0 (1.7 to 2.3)# | 2.6 (2.3 to 2.9)# |
| Peak late RVFPD, mm Hg | 0.5 (0.3 to 0.7)†‡ | 1.2 (1.0 to 1.4)‖ | 0.8 (0.6 to 0.9) | 0.7 (0.5 to 0.9) | 0.8 (0.7 to 1.0) | 0.6 (0.4 to 0.8)# | 1.0 (0.8 to 1.2)# |
| Peak early inertial RVFPD, mm Hg | 1.0 (0.8 to 1.2)*§ | 1.4 (1.2 to 1.6)¶ | 2.4 (2.1 to 2.7) | 1.9 (1.6 to 2.2) | 2.7 (2.4 to 3) | 2 (1.7 to 2.3) | 2.6 (2.3 to 2.9)# |
| Peak early convective RVFPD, mm Hg | 0.0 (−0.0 to 0.0) | 0.0 (−0.1 to 0.0) | −0.1 (−0.1 to 0.0) | −0.1 (−0.1 to 0.0) | −0.1 (−0.1 to 0.0) | −0.1 (−0.1 to 0.0) | −0.1 (−0.1 to 0.0) |
| Time to peak early RVFPD, % of filling | 7 (5 to 10) | 11 (7 to 14) | 6 (5 to 8) | 6 (4 to 8) | 7 (6 to 9) | 4 (3 to 6) | 9 (7 to 11)# |
| Time to peak late RVFPD, % of filling | 72 (68 to 76)* | 79 (75 to 83)¶ | 68 (65 to 71) | 70 (67 to 73) | 71 (68 to 74) | 70 (68 to 73) | 65 (62 to 68) |
| Time to peak early inertial RVFPD, % of filling | 7 (5 to 10) | 11 (8 to 14)‖ | 6 (5 to 8) | 6 (4 to 8) | 8 (6 to 9) | 4 (3 to 6) | 9 (7 to 11)# |
| Time to peak early convective RVFPD, % of filling | 11 (9 to 14)‡ | 13 (10 to 16)‖ | 7 (5 to 10) | 8 (5 to 10) | 11 (8 to 13)# | 7 (4 to 9) | 12 (9 to 14)# |

Data are presented as in Table 1, accounting for repeated measures within subject.

*$P<0.05$, †$P<0.01$, DCM vs age-matched control subjects; ‡$P=0.05$, §$P<0.0001$, DCM vs young volunteers at baseline; ‖$P\leq0.05$ and ¶$P<0.001$, age-matched control subjects vs young volunteers at baseline; #$P<0.05$, young volunteers vs baseline.

## Role of Inertial Forces as Determinants of the Physiological RVFPD

The present study characterizes, also for the first time, the fluid dynamics of the RV filling pressure gradient. Our results demonstrate that the RVFPD across the normal valve is caused almost exclusively by inertial forces; convective forces are irrelevant at this location.

Because viscosity is negligible at normal intracardiac flow ranges, intracardiac pressure differences result mostly from the combination of convective and inertial forces. In the presence of a restrictive orifice such as a tight valvular stenosis, convective forces predominate, and the pressure difference can be approximated by the simplified Bernoulli equation. However, as the valvular orifice diameter increases, the convective component decreases, and the inertial contribution to the total pressure difference becomes significant. The lack of contribution of convective forces to the RVFPD is related to the relatively low velocities present during RV filling and to the "hourglass" shape of the RA-RV inflow pathway. From the high RA to the RV apex, flow first undergoes a phase of convective acceleration as a result of geometric tapering of the fluid field along the tricuspid inlet.

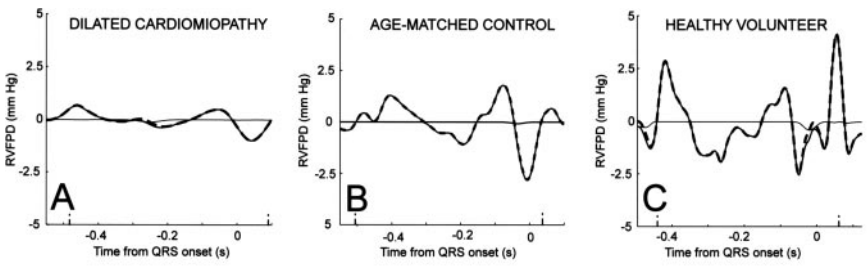


**Figure 3.** Representative example of RVFPD curve of a DCM patient (A), the 68-year-old control subject (B), and a 26-year-old volunteer (C). The thick solid line represents the total RVFPD; dotted and thin solid lines, the inertial and convective components, respectively. Notice that the total RVFPD line and inertial RVFPD are superimposed in the 3 examples.

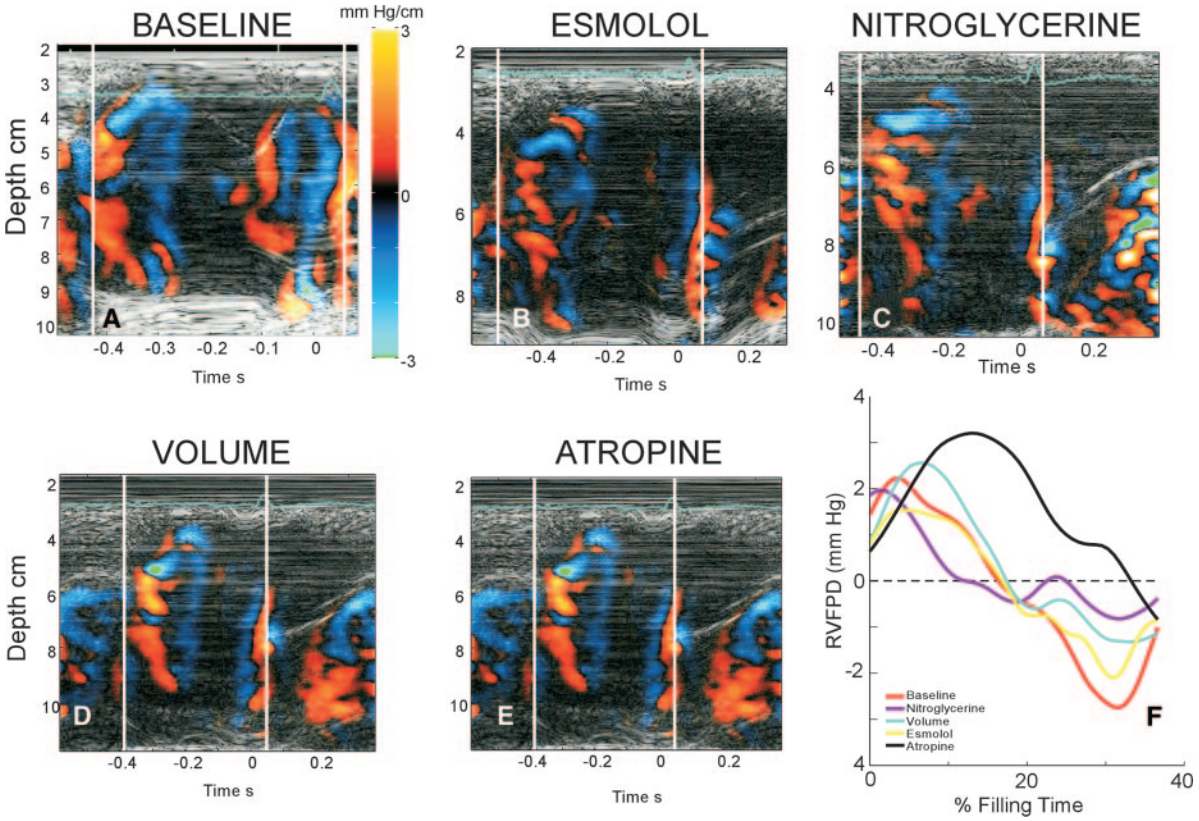


**Figure 4.** Examples of the effect of drug interventions on pressure gradients (A through E) and early RVFPDs (F) in a healthy volunteer normalized for the filling period.

But, as flow separates from the leaflet tips, the cross-sectional area of the right inflow field rapidly expands as it reaches the major diameter of the RV.[5] Consequently, intraventricular convective deceleration generates a negative pressure force that opposes filling, as previously described for the LV.[13] As a result, the effects of flow acceleration and deceleration cancel out when the total RA-to-RV-apex RVFPD is measured (Figure 5). It is noteworthy that this spatial distribution of the inflow field renders whatever method is used to quantify the RVFPD particularly sensitive to the place where the measuring stations are positioned.

The time-averaged ("mean") RVFPD was not significantly different from 0. Although this finding may seem striking, it must be noted that, as formulated in Euler's equation, the time average of the inertial component of the RVFPD (mean RVFPD) is 0 by definition.[26] Consequently, this finding from the catheterization data further confirms that inertial forces are almost the only force responsible for RV filling.

## Importance of Relaxation on RV Filling

A number of findings of our study emphasize the role of RV relaxation as a major determinant of RV filling. First, RVFPD values in DCM patients were 30% lower than in age-matched control subjects, and, in turn, the RVFPD was 40% lower in the age-matched control subjects than in healthy control subjects. Second, pharmacological interventions on the lusitropic state using esmolol significantly reduced the peak RVFPD in animals and healthy subjects. Finally, the analysis of hemodynamic correlates demonstrated that the peak RVFPD is determined by $\tau$. Because of its thin walls and low pressures, it could be hypothesized that the RV is filled passively. However, several studies have established a role of early diastolic suction as a determinant of RV filling during early diastole.[22,23,27] During this phase, the RV also is capable of lowering intracavitary pressure below RA values and continuing to decrease its pressure despite its increasing volume. The finding of our study of a peak RVFPD lower than the peak left-side equivalent (typically in the 3.5- to 4-mm Hg range) is probably explained by the slower relaxation rate of the RV compared with the LV.

## Clinical Applications

Strong evidence has emphasized the importance of RV function on prognosis in a number of cardiovascular diseases. Despite the fact that the methodologies of assessment are heterogeneous, it is now recognized that impaired RV systolic function is a major determinant of survival in patients suffering from ischemic[28] or idiopathic dilated cardiomyopathy.[28] In addition, RV function is among the most powerful predictors of long-term survival of patients with advanced heart failure, even more valuable than LV ejection fraction.[29] Importantly, these and other studies assessing the prognostic and clinical correlation of RV involvement have been based exclusively on markers of RV systolic performance (see elsewhere[1] for review). The few clinical studies that have analyzed RV diastolic function in the context of heart failure patients have been based on either the filling flow velocity profile[30,31] or

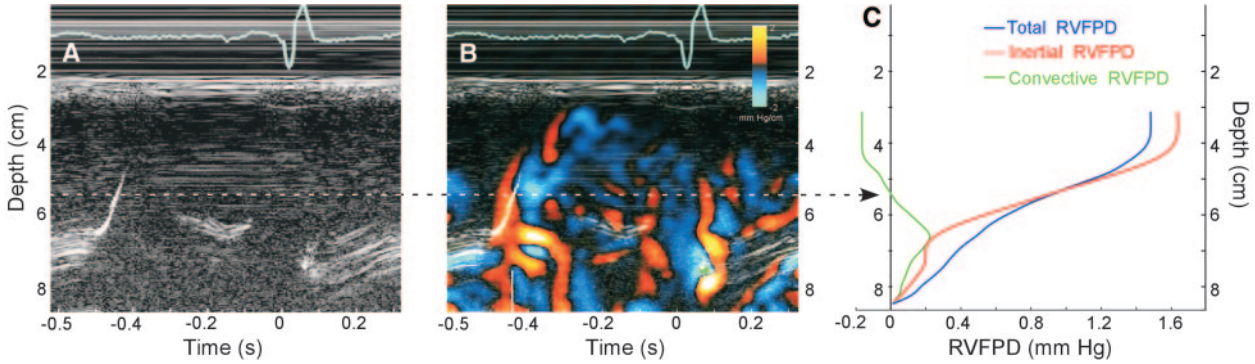


**Figure 5.** Spatial analysis of the generation of the RVFPD along the RV inlet. A, Gray-scale M-mode image; B, pressure gradient image; C, RVFPD spatial curves at the time of peak RVFPD (white vertical line in B). Note that the convective gradient contributes positively to the total RVFPD as blood accelerates toward the tricuspid valve. At the level of the tricuspid tips (white dotted horizontal line), the convective gradient changes its sign as a result of flow deceleration within the RV.

tissue Doppler measurements of regional RV myocardial velocity.[32] A high prevalence of RV diastolic abnormalities has been demonstrated with these methods in patients with heart failure.[31] By measuring the true driving force of filling, color Doppler M-mode processing allows us to characterize RV filling closer to its more elemental physiological properties. The observation of significantly reduced RVFPD values in patients with DCM, unmasking severely impaired relaxation in these patients, illustrates this advantage. Hypothetically, the RV $\tau$ could be quantified from the RVFPD with appropriate inverse regression equations because the other determinant factor, mean RA pressure, can be measured with relative accuracy with Doppler echocardiography.[20,33] Furthermore, it may be possible to adapt the method to measure right intraventricular diastolic suction, as we have demonstrated in the LV.[13]

Quantification of the mean RVFPD with the simplified Bernoulli equation is currently the most reliable method to assess the severity of tricuspid stenosis.[10] This method has been demonstrated to be reasonably accurate when Doppler and catheterization measurements are obtained simultaneously.[34,35] However, the present study demonstrates that by no means is the method suitable for estimating peak RVFPD. The study also demonstrates that, although baseline E-wave velocity correlates acceptably with the RVFPD between subjects at baseline, there is wide patient variability under changing hemodynamic conditions (different slopes shown in Figure 6); thus E-wave velocity is a suboptimal surrogate of the RVFPD.

## Study Limitations

Images from 3 volunteers and 2 patients were of insufficient quality for analysis. This observation suggests that the applicability of the method may be lower for measuring the RVFPD than in other intracardiac locations. A 2-dimensional plus time generalization of the method could be useful in

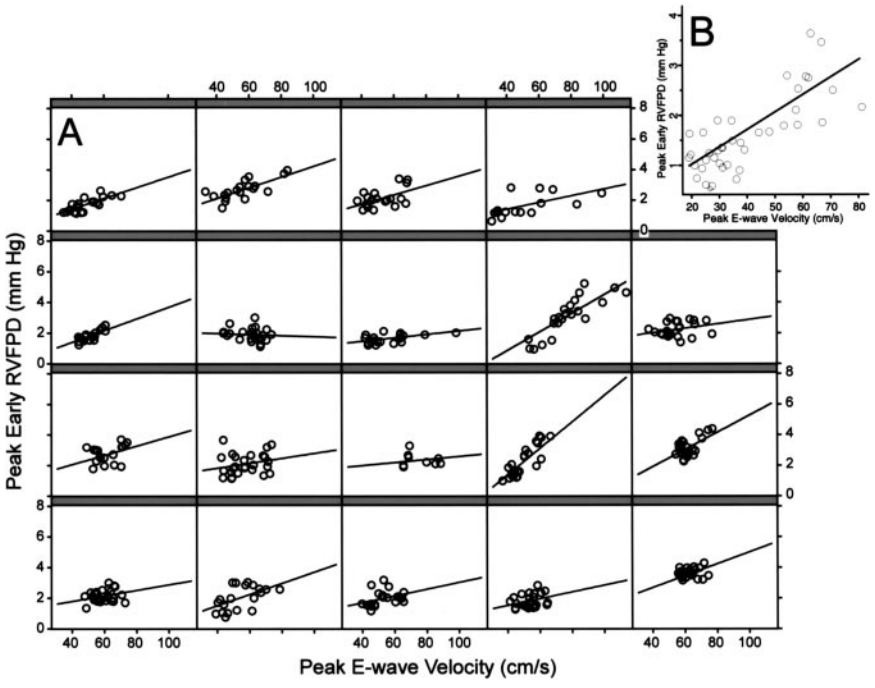


**Figure 6.** Within-subject (A; interventions on healthy volunteers) and between-subject (B; all populations, baseline values) relationships of the instantaneous RVFPD with the E-wave velocity. Within- and between-subject correlation coefficients are $R=0.77$ and $R=0.73$, respectively.

those cases in which RV filling flow deviates most from the straight streamline assumption.

The low magnitude of the measured RVFPD is probably close to the resolution of the high-fidelity micromanometers. However, this is the best method available for direct validation of intracardiac pressure measurements. A functional image processing approach has been demonstrated to provide the distributions of pressure differences inside the RV.[7] This technique requires very high-resolution measurements of the endocardial boundaries in 3-dimensional plus time and complex processing, which were beyond the scope of this article. However, it is noteworthy that both the magnitude and waveforms of the RVFPD curves reported with this methodology[7] closely resemble our findings.

Importantly, each animal underwent more than a single intervention. Because baseline data were not reacquired before each stage, the statistical significance of the effects of hemodynamic changes (Table 1) must be interpreted with caution. A number of factors are known to modify RV filling (eg, closed versus intact pericardium, spontaneous versus mechanical ventilation, or awake versus sedated state). Assessing the impact of these factors on the RVFPD deserves specific studies. Additionally, application of this new method in patients with known RV disease from chronic or pressure overload is warranted.

### Conclusions

For the first time, the RV driving filling force can be accurately measured noninvasively in the clinical setting. The method is sensitive to detect the effects of preload, chronotropic, and lusitropic states on filling dynamics. The RV filling force is reduced in patients with DCM, indicating impaired RV relaxation in this disease. These findings suggest that the noninvasive measurement of the RVFPD is a useful tool for the clinical assessment of RV diastolic function.

## Acknowledgments

We are indebted to the personnel from the Unit of Experimental Medicine and Surgery of the Hospital General Universitario Gregorio Marañón for their assistance and to General Electric Healthcare for providing equipment support for the study.

## Sources of Funding

The present study was supported by Ministerio de Sanidad y Consumo–Instituto de Salud Carlos III (Spain) grants PI061101, CM06/00085 (to Dr Cortina), and RECAVA. Dr Garcia is supported by the Natural Sciences and Engineering Research Council of Canada (NSERC No. 306188).

## Disclosures

Dr Bermejo has received research equipment support from General Electric Healthcare for the present study. The other authors report no conflicts.

## References

1. Voelkel NF, Quaife RA, Leinwand LA, Barst RJ, McGoon MD, Meldrum DR, Dupuis J, Long CS, Rubin LJ, Smart FW, Suzuki YJ, Gladwin M, Denholm EM, Gail DB. Right ventricular function and failure: report of a National Heart, Lung, and Blood Institute Working Group on Cellular and Molecular Mechanisms of Right Heart Failure. *Circulation*. 2006; 114:1883–1891.
2. Di Salvo TG, Mathier M, Semigran MJ, Dec GW. Preserved right ventricular ejection fraction predicts exercise capacity and survival in advanced heart failure. *J Am Coll Cardiol*. 1995;25:1143–1153.
3. Lee FA. Hemodynamics of the right ventricle in normal and disease states. *Cardiol Clin*. 1992;10:59–67.
4. Pasipoularides A, Shu M, Shah A, Silvestry S, Glower DD. Right ventricular diastolic function in canine models of pressure overload, volume overload, and ischemia. *Am J Physiol Heart Circ Physiol*. 2002;283: H2140–H2150.
5. Pasipoularides A, Shu M, Shah A, Tucconi A, Glower DD. RV instantaneous intraventricular diastolic pressure and velocity distributions in normal and volume overload awake dog disease models. *Am J Physiol Heart Circ Physiol*. 2003;285:H1956–H1965.
6. Pasipoularides A, Shu M, Shah A, Womack MS, Glower DD. Diastolic right ventricular filling vortex in normal and volume overload states. *Am J Physiol Heart Circ Physiol*. 2003;284:H1064–H1072.
7. Pasipoularides AD, Shu M, Womack MS, Shah A, Von Ramm O, Glower DD. RV functional imaging: 3-D echo-derived dynamic geometry and flow field simulations. *Am J Physiol Heart Circ Physiol*. 2003;284: H56–H65.
8. Thomas JD, Newell JB, Choong CY, Weyman AE. Physical and physiological determinants of transmitral velocity: numerical analysis. *Am J Physiol*. 1991;260:H1718–H1731.
9. Choong CY, Abascal VM, Thomas JD, Guerrero JL, McGlew S, Weyman AE. Combined influence of ventricular loading and relaxation on the transmitral flow velocity profile in dogs measured by Doppler echocardiography. *Circulation*. 1988;78:672–683.
10. Weyman AE. Right ventricular inflow tract. In: Weyman AE, ed. *Principles and Practice of Echocardiography*. Philadelphia, Pa: Lea & Febiger; 1994:824–862.
11. Yotti R, Bermejo J, Antoranz JC, Rojo-Alvarez JL, Allue C, Silva J, Desco MM, Moreno M, Garcia-Fernandez MA. Noninvasive assessment of ejection intraventricular pressure gradients. *J Am Coll Cardiol*. 2004; 43:1654–1662.
12. Bermejo J, Antoranz JC, Yotti R, Moreno M, Garcia-Fernandez MA. Spatio-temporal mapping of intracardiac pressure gradients: a solution to Euler's equation from digital postprocessing of color Doppler M-mode echocardiograms. *Ultrasound Med Biol*. 2001;27:621–630.
13. Yotti R, Bermejo J, Antoranz JC, Desco MM, Cortina C, Rojo-Alvarez JL, Allue C, Martin L, Moreno M, Serrano JA, Munoz R, Garcia-Fernandez MA. A noninvasive method for assessing impaired diastolic suction in patients with dilated cardiomyopathy. *Circulation*. 2005;112: 2921–2929.
14. Yotti R, Bermejo J, Desco MM, Antoranz JC, Rojo-Alvarez JL, Cortina C, Allue C, Rodriguez-Abella H, Moreno M, Garcia-Fernandez MA. Doppler-derived ejection intraventricular pressure gradients provide a reliable assessment of left ventricular systolic chamber function. *Circulation*. 2005;112:1771–1779.
15. Firstenberg MS, Vandervoort PM, Greenberg NL, Smedira NG, McCarthy PM, Garcia MJ, Thomas JD. Noninvasive estimation of transmitral pressure drop across the normal mitral valve in humans: importance of convective and inertial forces during left ventricular filling. *J Am Coll Cardiol*. 2000;36:1942–1949.
16. Greenberg NL, Vandervoort PM, Thomas JD. Instantaneous diastolic transmitral pressure differences from color Doppler M mode echocardiography. *Am J Physiol*. 1996;271:H1267–H1276.
17. Pasipoularides A. Clinical assessment of ventricular ejection dynamics with and without outflow obstruction. *J Am Coll Cardiol*. 1990;15: 859–882.
18. Pasipoularides AD, Shu M, Shah A, Glower DD. Right ventricular diastolic relaxation in conscious dog models of pressure overload, volume overload, and ischemia. *J Thorac Cardiovasc Surg*. 2002;124:964–972.
19. Ghio S, Recusani F, Klersy C, Sebastiani R, Laudisa ML, Campana C, Gavazzi A, Tavazzi L. Prognostic usefulness of the tricuspid annular plane systolic excursion in patients with congestive heart failure secondary to idiopathic or ischemic dilated cardiomyopathy. *Am J Cardiol*. 2000;85:837–842.
20. Kircher BJ, Himelman RB, Schiller NB. Noninvasive estimation of right atrial pressure from the inspiratory collapse of the inferior vena cava. *Am J Cardiol*. 1990;66:493–496.
21. Edwards D, Berry JJ. The efficiency of simulation-based multiple comparisons. *Biometrics*. 1987;43:913–928.
22. Sabbah HN, Anbe DT, Stein PD. Can the human right ventricle create a negative diastolic pressure suggestive of suction? *Cathet Cardiovasc Diagn*. 1981;7:259–267.

23. Sabbah HN, Stein PD. Negative diastolic pressure in the intact canine right ventricle: evidence of diastolic suction. *Circ Res*. 1981;49:108–113.
24. Courtois M, Barzilai B, Gutierrez F, Ludbrook PA. Characterization of regional diastolic pressure gradients in the right ventricle. *Circulation*. 1990;82:1413–1423.
25. Killip T 3rd, Lukas DS. Tricuspid stenosis; physiologic criteria for diagnosis and hemodynamic abnormalities. *Circulation*. 1957;16:3–13.
26. Clark C. The fluid mechanics of aortic stenosis, I: theory and steady flow experiments. *J Biomech*. 1976;9:521–528.
27. Sun Y, Belenkie I, Wang JJ, Tyberg JV. Assessment of right ventricular diastolic suction in dogs using wave-intensity analysis. *Am J Physiol Heart Circ Physiol*. 2006;291:H3114–H3121.
28. Polak JF, Holman BL, Wynne J, Colucci WS. Right ventricular ejection fraction: an indicator of increased mortality in patients with congestive heart failure associated with coronary artery disease. *J Am Coll Cardiol*. 1983;2:217–224.
29. Karatasakis GT, Karagounis LA, Kalyvas PA, Manginas A, Athanassopoulos GD, Aggelakas SA, Cokkinos DV. Prognostic significance of echocardiographically estimated right ventricular shortening in advanced heart failure. *Am J Cardiol*. 1998;82:329–334.
30. Henein MY, O'Sullivan CA, Coats AJ, Gibson DG. Angiotensin-converting enzyme (ACE) inhibitors revert abnormal right ventricular filling in patients with restrictive left ventricular disease. *J Am Coll Cardiol*. 1998;32:1187–1193.
31. Yu CM, Sanderson JE, Chan S, Yeung L, Hung YT, Woo KS. Right ventricular diastolic dysfunction in heart failure. *Circulation*. 1996;93:1509–1514.
32. Spinarova L, Meluzin J, Toman J, Hude P, Krejci J, Vitovec J. Right ventricular dysfunction in chronic heart failure patients. *Eur J Heart Fail*. 2005;7:485–489.
33. Nagueh SF, Kopelen HA, Zoghbi WA. Relation of mean right atrial pressure to echocardiographic and Doppler parameters of right atrial and right ventricular function. *Circulation*. 1996;93:1160–1169.
34. Perez JE, Ludbrook PA, Ahumada GG. Usefulness of Doppler echocardiography in detecting tricuspid valve stenosis. *Am J Cardiol*. 1985;55:601–603.
35. Fawzy ME, Mercer EN, Dunn B, al-Amri M, Andaya W. Doppler echocardiography in the evaluation of tricuspid stenosis. *Eur Heart J*. 1989;10:985–990.

## CLINICAL PERSPECTIVE

Right ventricular (RV) function is known to be a major determinant of outcome in a number of cardiovascular disease states. Outcome research on the RV has focused almost exclusively on systolic function because the diastolic properties of the RV remain scarcely studied in the clinical setting. The driving force for RV filling (the diastolic pressure gradient from the right atrium to the apex, the RV filling pressure difference) has never been measured in the clinical setting. Recently, the accuracy of measuring pressure gradients by processing color-Doppler M-mode images has been demonstrated in other intracardiac locations. First, the present study validates in a high-fidelity experimental setup this method for measuring the RV filling pressure difference. Next, under well-controlled experimental conditions, the present study shows that the RV filling pressure difference depends nonlinearly on right atrial pressure and directly on the rate of RV relaxation. Finally, application in 3 clinical populations (healthy volunteers, dilated cardiomyopathy patients, and age-matched control subjects) shows that the RV filling pressure difference measured noninvasively is a sensitive tool for detecting changes in RV preload, chronotropic, and lusitropic states. Interestingly, a severe impairment in diastolic function is demonstrated in dilated cardiomyopathy patients. By accounting for the true force responsible for filling, the study introduces a new noninvasive method for characterizing RV diastolic function closer to its more elemental physiological properties. Future studies assessing the clinical value of this method in terms of functional status and outcome in other populations with subclinical RV disease or overt RV dysfunction resulting from pressure or volume overload are warranted.